Published in final edited form as:
Brain Struct Funct. 2012 April ; 217(2): 435–446. doi:10.1007/s00429-011-0342-9.

Sensory deprivation differentially impacts the dendritic development of pyramidal versus non-pyramidal neurons in layer 6 of mouse barrel cortex

Chia-Chien Chen,
Neuropsychology Doctoral Subprogram, The Graduate Center, CUNY, 365 Fifth Avenue, New York, NY 10016, USA

Danny Tam, and
Neuropsychology Doctoral Subprogram, The Graduate Center, CUNY, 365 Fifth Avenue, New York, NY 10016, USA

Joshua C. Brumberg
Neuropsychology Doctoral Subprogram, The Graduate Center, CUNY, 365 Fifth Avenue, New York, NY 10016, USA

Department of Psychology, Queens College, CUNY, 65-30 Kissena Boulevard, Flushing, NY 11367, USA

Joshua C. Brumberg: Joshua.brumberg@qc.cuny.edu

Abstract

Early postnatal sensory experience can have profound impacts on the structure and function of cortical circuits affecting behavior. Using the mouse whisker-to-barrel system we chronically deprived animals of normal sensory experience by bilaterally trimming their whiskers every other day from birth for the first postnatal month. Brain tissue was then processed for Golgi staining and neurons in layer 6 of barrel cortex were reconstructed in three dimensions. Dendritic and somatic parameters were compared between sensory-deprived and normal sensory experience groups. Results demonstrated that layer 6 non-pyramidal neurons in the chronically deprived group showed an expansion of their dendritic arbors. The pyramidal cells responded to sensory deprivation with increased somatic size and basilar dendritic arborization but overall decreased apical dendritic parameters. In sum, sensory deprivation impacted on the neuronal architecture of pyramidal and non-pyramidal neurons in layer 6, which may provide a substrate for observed physiological and behavioral changes resulting from whisker trimming.

Keywords

Neocortex layer 6; Golgi; Neuronal morphology; Barrel cortex; Sensory deprivation; Dendrites

Introduction

One of the fundamental features of the cerebral cortex is its remarkable ability to adapt to the sensory environment via, physiological, structural, genetic, and/or biochemical changes (for reviews see Buonomano and Merzenich 1998; Sur and Rubenstein 2005; Feldman and

Correspondence to: Joshua C. Brumberg, Joshua.brumberg@qc.cuny.edu.

Brecht 2005; Fox and Wong 2005). In the primary somatosensory cortex, such adaptations have been observed in alterations of cortical areal patterning, cytoarchitecture, neuronal physiology, and animal behavior, all resulting from significant disruptions in sensory experience during postnatal development (Van Der Loos and Woolsey 1973; Simons and Land 1987; Carvell and Simons 1996; Maravall et al. 2004; Zuo et al. 2005; McRae et al. 2007; Bruno et al. 2009; Hardingham et al. 2008; Takasaki et al. 2008; Briner et al. 2010; Popescu and Ebner 2010). A particular interest is the reorganization of dendritic arborizations following alterations in sensory experience and cellular activity. For example, it has been demonstrated in the visual system that following monocular deprivation, the dendritic fanning of layer 4 (L4) spiny stellate cells showed directional preference toward the innervated ocular dominance column while simultaneously avoiding the deprived cortical column (Kossel et al. 1995). Similarly in the whisker-to-barrel system, blocking cellular activity by knocking out a subunit of the cortical glutamate receptor resulted in dendritic fanning with significant areal overlap and crossings into the neighboring L4 barrels (Datwani et al. 2002), a phenomenon not observed in wild-type animals. In addition, this change in dendritic cytoarchitecture is not limited to L4, the main recipient zone of thalamocortical afferents, but is also observed in the overlying layer 3 pyramidal cells whose basilar dendrites reach into L4 (Maravall et al. 2004). In the adult cerebral cortex, it has been suggested that neuronal morphology is more stable and therefore requires considerably more dramatic measures such as peripheral lesions to induce dendritic reorganizations (Trachtenberg et al. 2002; Hickmott and Steen 2005; Tailby et al. 2005).

Despite the focus on the effects of sensory experience on neuronal architecture in the principal thalamic recipient zone (L4), surprisingly little data are available on its influence on pattern formation of dendrites originating from layer 6 (L6) neurons, which also receive direct thalamic input. Developmentally, L6 is the earliest cortical layer to differentiate from the ventricular zone, with the glutamatergic pyramidal cells being the first neurons to move into position in the cortical plate (for reviews see Rakic 2009; Thomson 2010). Anatomically, L6 also provides an abundance of projections to diverse regions such as the thalamus, multiple cortical areas, basal ganglia, claustrum, and the spinal cord (for review see Thomson 2010). This strategic anatomical positioning and wealth of connectivity suggest that this deepest cortical layer plays roles in multiple cortical functioning such as memory, object recognition, perceptual adjustment/gain control, sensori-motor integration, hemispheric balancing and, perhaps ultimately, consciousness (Katz 1987; Sherman and Guillery 2002; Crick and Koch 2005; Andolina et al. 2007; Rocco and Brumberg 2007; Ramos et al. 2008; Denton et al. 2009; López-Aranda et al. 2009; also see Thomson 2010). Therefore, it is of great interest to understand how disruptions of sensory experience during development may potentially impact on the structure, and in turn functioning, of L6.

The present study investigated the alterations of L6 neuronal structures that resulted from chronic sensory deprivation in developing animals. Sensory deprivation was induced via whisker trimming as has been done previously (Simons and Land 1987; McRae et al. 2007) and, in combination with our recently developed morphometric analyses (Chen et al. 2009), we reconstructed Golgi-impregnated neurons and quantified morphological changes of somata, and apical and basilar dendrites of pyramidal and non-pyramidal cells.

Materials and methods

Experimental animals and chronic sensory deprivation

The selection and treatment of experimental animals were followed exactly as previously described (McRae et al. 2007) and in accordance with the Queens College, CUNY Institutional Animal Care and Use Committee and NIH guidelines. Briefly, each animal from a litter of CD-1 mice was randomly assigned at birth to be either in the control ($n = 4$)

or sensory-deprived (n = 4, whisker trim) condition. For the sensory-deprived animals, the whiskers were manually clipped by precision microscissors as close to the base of the follicle as possible every other day for the first 30 postnatal days. At postnatal day P30/P31, brief administration (~ 1 min) of anesthesia (5% isoflurane, Aerrane) was done from postnatal day 14 to prevent the animals from moving during the trimming procedure. The within-litter control method was followed: all animals were exposed to the same conditions such as bedding texture, food and water source, maternal influence, anesthesia, handling, etc. The control animals were handled, anesthetized, and returned to the cage on the same trimming session as the sensory-deprived animals.

Golgi staining procedure and tissue processing

Brains were processed with our Golgi protocol as previously described (Chen et al. 2009), with minor modifications. In brief, after the establishment of anesthesia (0.3 ml Euthasol per animal, Henry Schein Inc.), brains were immediately removed, rinsed with double distilled water, and transferred to a Golgi-Cox solution composed of potassium dichromate, mercuric chloride, and potassium chromate that comes bundled with the FD Rapid GolgiStain™ Kit (FD Neurotechnologies, Inc.). The brains were stored at room temperature for 12–14 days in a glass bottle and transferred to a cryoprotectant solution stored at 4μC for at least another week in the dark. The brains were next rapidly frozen with dry ice and quickly embedded in Neg-50™ (Thermo Scientific, Inc), and cut into 180–200 μm sections in the coronal plane with a freezing cryostat. This section thickness was chosen by test-and-trial basis for optimized optical clarity of dendrites while simultaneously preserving the integrity of neuronal morphology. Sections were transferred onto triple-coated gelatin-dipped slides, and allowed to air dry at room temperature in the dark for approximately 4–5 days. Following drying, sections were rehydrated with double distilled water, reacted in a developing solution (FD Neurotechnologies, Rapid Golgi Stain Kit), and dehydrated with 50, 75, 95, and 100% ethanol, respectively. Finally, sections were defatted in xylene substitute (Manufacturer) and coverslipped using Permount (Fisher Scientific). Golgi staining was chosen as it is a standard method to investigate the qualitative and morphometric properties of neurons in the cerebral cortex (Lorente de Nó 1949; Woolsey et al. 1975; White 1978; Harris and Woolsey 1981; Lund and Wu 1997; Prieto and Winer 1999; Chen et al. 2009; Tran et al. 2009) and was well suited to our needs to fully label a subset of neurons in barrel cortex.

Cell selection, reconstruction, morphometric quantification, and statistical analyses

S1 barrel cortex was located by identifying the characteristic clusters of cells that are typically found in granular, supragranular, and infragranular layers (Fig. 1a, b) and by comparing with an atlas of a Golgi-stained mice brain (Valverde 1998). Neuronal somata and dendritic arborizations were examined and carefully reconstructed using an Olympus BX51 microscope with a 60× (oil immersion, NA 1.4) objective. The scope was equipped with a digital camera (Microfire, Optronics, Inc.), a mechanical stage (Ludl, Thornwood, NY), and an x–y–z axis encoder connected to a Windows Pentium-4 PC. Neurolucida software (version 8.0 by MBF Bioscience, Inc.) was used to visualize and manually reconstruct the cell bodies and dendrites as closely as possible (see Fig. 1c–f). Only the neurons that exhibited complete Golgi impregnation without significant staining artifacts were selected for reconstruction. Since the role of atypically oriented (e.g., inverted) pyramidal neurons is still unclear and might be rather heterogeneous (Mendizabal-Zubiaga et al. 2007; Chen et al. 2009), the pyramidal cells that exhibited atypical orientation were excluded from our reconstructions. While it is a possibility that some extremely long dendrites may be truncated during the tissue sectioning and preparation process, we aimed to reconstruct neurons whose apical dendrites came to a tapered point without any noticeable bleb. Any neurons with dendrites that were suspected to be truncated were eliminated from

our sampling pool. NeuroExplorer (MBF Bioscience, Inc.) was used to quantify numerous morphological measurements (see Tables 1, 2, and section " Results"), as previously described (Chen et al. 2009). The explored morphological characteristics included somatic shape and size, dendritic structure, branching patterns, and Sholl analysis (Sholl 1956). Sholl analyses data were gathered, and we performed mixed-factorial analyses of variance (ANOVA), followed by appropriate post hoc confirmations (Tukey HSD/Fisher LSD tests). We quantified approximately ~35 morphological variables per reconstructed neuron (see Tables 1, 2 and section " Results") and treated each neuron as an individual case (see Chen et al. 2009). We then performed parametric pair-wise comparisons (two-tailed independent group *t* test) between the control and sensory-deprived groups due to the relatively comparable number of neurons across groups.

Results

We previously reported that L6 neurons (as defined by somata located between the white matter and L5, using large L5 pyramidal neurons to mark the superficial L5–L6 border, see Chen et al. 2009) in the S1 barrel field can be morphologically classified into two distinct categories: those with and without apical dendrites (e.g., pyramidal and non-pyramidal cell types; Chen et al. 2009). For the present study, we therefore divided L6 neurons into these two categories as well, and performed corresponding morphometric analyses in the sensory-deprived versus control conditions in these two groups of neurons. Since the conditions were held constant (handling of animals, anesthesia, tissue processing methodologies, tissue sectioning thickness, etc.), we propose that the observed differences in morphological variables are most likely due to the effect of peripheral sensory deprivation from birth.

Effect of chronic sensory deprivation on dendritic arborizations of non-pyramidal neurons

The results of our morphometric quantification of non-pyramidal neurons (sensory deprived $n = 21$ neurons, control $n = 35$ neurons, all data are expressed as per neuron unless otherwise noted) suggested that the shape of the somata was not significantly affected by chronic sensory deprivation (statistically non-significant for all 10 investigated somatic variables). In contrast, we observed several significant changes in the dendritic components of these non-pyramidal neurons as a result of chronic sensory deprivation (see Table 1; Figs. 2b, d, 3a). Overall, with exception of the primary dendritic quantity (defined as the number of dendritic trunks sprouting from somata), which did not significantly vary between conditions, all other dendritic components were significantly elevated in the animals that experienced chronic sensory deprivation compared to control animals ($p < 0.05$). These dendritic components included the number of dendritic nodes (bi- or trifurcations per neuron), dendritic ends, dendritic length, mean dendritic length (per dendrite per neuron), total dendritic surface area, mean surface area (per dendrite per neuron), dendritic volume, and dendritic mean volume (per dendrite per neuron). The non-pyramidal neurons of animals that experienced chronic sensory deprivation showed increased total length of dendritic trees as well as increased number of higher order (non-primary) dendritic branches. Results from our Sholl analyses (between-groups ANOVA; post hoc: Tukey HSD tests, $p < 0.05$) showed that the changes were in dendritic segments between 30 and 90 μm from the soma, with significant increases seen in the number of intersections and increases in dendritic length in this region of the dendritic arbor. The unchanged segments are the immediately proximal (<30 μm from the soma) and the distal segments of the dendritic tree (>100 μm for dendritic intersections and >120 μm for dendritic length, see Fig. 3b, c). This pattern of data suggests that sensory deprivation does not significantly influence the proximal cellular architecture components of L6 non-pyramidal neurons. These results are consistent with our findings that there were no changes in any of the somatic parameters, in the number of primary dendritic trees, or number of immediate proximal dendritic segments. However, the effect of chronic

sensory deprivation on the intermediate neuronal regions is evident, as indicated by the increased number of bi/trifurcations and dendritic ends, which are indicators that there was more dendritic branching in this region of the cell's dendritic tree (see Table 1). The results of our Sholl analyses further supported the finding that the intermediate dendritic areas are largely affected as well (Fig. 3b, c).

Effect of chronic sensory deprivation on pyramidal neurons

The somata of pyramidal neurons, unlike the non-pyramidal neurons, were affected by chronic sensory deprivation from birth. It was observed that soma perimeter, area, and feret maximum (longest axis of the soma) and minimum (longest axis perpendicular to the feret maximum) were considerably increased in the sensory-deprived condition compared to the control animals (sensory deprived $n = 39$ neurons, control $n = 35$ neurons). Other somatic factors that indicated the intrinsic shape of the somata (aspect ratio, compactness, convexity, form factor, roundness, solidity; for descriptions see Table 1) were not significantly affected (Table 2). This suggests that while there is a proportional increase of somata size following sensory deprivation, the fundamental geometric shapes of the pyramidal neuronal type were unchanged (i.e., sensory deprivation did not alter the triangular somata of pyramidal neurons into spherical ones).

Apical and basilar dendrites of the L6 pyramidal neurons responded to chronic sensory deprivation in opposite ways (see Fig. 2a, c). The apical dendrites in the sensory-deprived mice showed significant decrease in a variety of related parameters, including apical dendritic nodes, apical dendritic ends, apical dendritic length, apical dendritic surface area, and apical dendritic volume (Fig. 4a, also see Table 2). Detailed investigation using Sholl analyses (between-groups ANOVA; post hoc: Fisher LSD, $p < 0.05$) on apical dendritic intersection and apical dendritic length indicated that these differences were predominantly distal to the somata (see Fig. 4b, c), suggesting that this significant decrease of apical dendritic features most likely occurred outside of L6. In sum, these findings are consistent with an overall retraction of the apical dendrite.

In contrast to the overall decrease of apical dendritic components, the basilar dendritic components showed significant increases in their dendritic span (Fig. 5a, also see Table 2), exemplified by elevated basilar dendritic nodes, basilar dendritic ends, and basilar dendritic length (between-groups ANOVA; post hoc: Fisher LSD, $p < 0.05$). Even though the increase might not be as robust as in the nonpyramidal neurons, the overall trend still suggested that the basilar dendritic features of pyramidal neurons experienced significant expansion. Further examination with the Sholl analyses revealed that similar to the non-pyramidal neurons, this increase in basilar dendritic arborization is mostly observed in the intermediate-to-proximal region (Fig. 5b, c), indicating that its effect is generally confined to L6. Lastly, the total dendritic (apical + basilar) components showed no significant change, including total dendritic quantity, nodes, ends, length, surface area, and volume, indicating that there might be homeostatic mechanisms of dendritic morphology similar to that previously proposed (Samsonovich and Ascoli 2006). Taken together, our data suggest that apical and basilar dendritic components responded to chronic sensory deprivation in opposite fashions; however, these changes counterbalance each other resulting in no significant change in the total dendritic components.

Discussion

The goal of the current research was to describe the effect of chronic sensory deprivation on the development of neuronal morphologies, specifically in somatic, apical dendritic, and basilar dendritic components in the neocortical L6. The rodent whisker-to-barrel cortex is an ideal system to study the impact of sensory experience on neuronal morphology due the ease

of inducing sensory deprivation and correlating it with known anatomical structures (see Fox and Wong 2005; Feldman and Brecht 2005; Petersen 2007). We utilized the Golgi impregnation procedure which reduces possible bias in labeling neurons (Pasternak and Woolsey 1975). A limitation of this particular staining technique is that one cannot assign a specific functional class of the neuronal type labeled, other than pyramidal versus non-pyramidal neurons based on the presence or lack of apical dendritic features (Chen et al. 2009). Since the observation of the morphological change in somata and dendrites were made post-manipulation (control vs. sensory deprived), we cannot rule out the possibility that there were phenotypic specific changes in morphology. It may be particularly rewarding for future studies to discern the effect of chronic sensory deprivation on specific functional neurons in this understudied layer of the cerebral cortex (e.g., the effect of chronic sensory deprivation on cortical–thalamic neurons).

Our data suggest that neurons in L6 of the barrel cortex indeed respond to chronic sensory deprivation by altering their somata (in case of pyramidal neurons) and dendritic architectures during development. While the somata of non-pyramidal neurons do not respond to chronic sensory deprivation, their dendrites are dramatically affected and show a significant increase in almost every dendritic variable investigated. In pyramidal neurons, key somatic structures such as perimeter, area, feret maximum, and feret minimum showed significant elevation following chronic sensory deprivation, and the apical and basilar dendrites of L6 pyramidal neurons responded differentially. Apical dendrites showed an overall trend to decrease following chronic sensory deprivation, while basilar dendrites showed an overall trend to increase.

It has been previously demonstrated in the primate striate cortex that chronic dark rearing from birth induced the expansion of dendritic fields (Neal et al. 1985). Also, a recent study in the whisker-to-barrel system showed that brief sensory deprivation at birth (for 3 days) led to increased dendritic span in L4 spiny stellate cells (Lee et al. 2009). Here, our data provide evidence that a similar phenomenon is also observed in developing L6 of the rodent somatosensory cortex, in which significant changes in dendritic arborizations result from chronic sensory deprivation. In addition, we show that this effect exists in both pyramidal and non-pyramidal neurons, with its effect more pronounced in non-pyramidal cells. Within the developmental period, it is known that the dendrites of L6 neurons dramatically increase in both number and length during the first several weeks after birth, followed by massive dendritic pruning (Lübke and Albus 1989). This study also showed that the size of somata mimicked a similar pattern. One possible explanation of our results is that chronic sensory deprivation has stunted the dendritic pruning process, leading to comparatively elevated dendritic parameters such as increased dendritic length, ends, surface area, and volume that are reported here. This idea has been previously proposed (Bestman et al. 2008) and is consistent with the finding that dark rearing delays the dendritic pruning process (Tian and Copenhagen 2003). While the exact mechanism is unknown, it has been shown that there are decreases in NMDA receptor activation following trimming (Zuo et al. 2005) and this has been shown to play a crucial role in dendritic development (reviewed in Cline and Haas 2008). Likewise in the present study, chronic sensory deprivation resulted in increased somata size and dendritic field, suggesting that sensory deprivation delays experience-dependent changes in both dendritic and soma maturation.

Physiological studies have shown that there is a shift in the balance of excitatory/inhibitory cortical networks following chronic sensory deprivation (Lee et al. 2007; Marik et al. 2010; Sun 2009). This shift in balance is exemplified by the excitatory regular spiking units (RSUs) and the inhibitory fast spiking units (FSUs) responding in different ways following chronic sensory deprivation (Lee et al. 2007; Sun 2009). The increased expression of parvalbumin in GAB-Aergic neurons and associated decrease of the perineuronal net

expression have been proposed to be responsible for this sensory deprivation-induced network shift (Jiao et al. 2006; McRae et al. 2007). The net result is increased activity in response to whisker stimulation within L4 and decreases in signal-to-noise ratio (Simons and Land 1987), which may underlie the finding that deprived animals have poorer discriminatory abilities (Carvell and Simons 1996).

Our findings add to the growing body of knowledge that the cerebral cortex adapts to environmental manipulations in a layer-specific fashion (Oray et al. 2004; Lee et al. 2007) and, based on the present data, in a cell-specific manner as well. The differences in reorganization of the apical and basilar dendrites of pyramidal neurons are reminiscent to what is seen in response to chronic stress (Garrett and Wellman 2009). This type of cellular homeostasis in which that apical and basilar dendrites respond in opposite fashion following stress has been proposed and demonstrated previously (Samsonovich and Ascoli 2006). Our finding suggests that dendrites do not function as an independent unit within a cell, but rather are coordinated: when the source of sensory input is limited, other dendrites may look for active inputs to compensate for the optimal activity that the neurons need, perhaps to survive. This is further highlighted by our data that total (apical + basilar) dendritic components of L6 pyramidal neurons do not show a significant difference following trimming, even though apical or basilar components show a significant difference in opposite directions.

Morphology impacts the input/output relationship of neurons (Mainen and Sejnowski 1996; Krichmar et al. 2002). In particular, it has been shown that inputs that are located distant from the soma (e.g., on an apical dendrite) can be attenuated/filtered (Rall and Rinzel 1973, Komendantov and Ascoli 2009). Furthermore, dendritic branching patterns impact coincidence detection (Schaefer et al. 2003) and have been hypothesized to impact on the firing properties of the neuron itself (Mainen and Sejnowski 1996; van Ooyen et al. 2002). Thus, changes in dendritic parameters, as observed in the present study, are likely to impact on the neurons' ability to integrate incoming signals and alter their firing patterns. The end result would be changes to responses to incoming afferent signals (e.g., from the whiskers), which have been observed in vivo in layer 4 following trimming (Simons and Land 1987).

Our findings have provided further evidence that cortical neurons indeed respond to changes in sensory activation by reorganizing cellular resources in the form of morphological remodeling, most likely to keep the homeostatic balance within the affected neuronal network.

Acknowledgments

The work was supported by a DSC award to C.-C. Chen and PSC-CUNY 62750-00 40 and NS058758 to J.C.B. We thank Dr.'s Raddy L. Ramos and Carolyn Pytte for helpful comments on the manuscript.

References

Andolina IM, Jones HE, Wang W, Sillito AM. Corticothalamic feedback enhances stimulus response precision in the visual system. PNAS. 2007; 104(5):1685–1690. [PubMed: 17237220]

Bestman, J.; Santos da Silva, J.; Cline, HT. Dendrite development. In: Stuart, G.; Spruston, N.; Häusser, M., editors. Dendrites. NY: Oxford University Press; 2008. p. 35-67.

Briner A, De Roo M, Dayer A, Muller D, Kiss JZ, Vutskits L. Bilateral whisker trimming during early postnatal life impairs dendritic spine development in the mouse somatosensory barrel cortex. J Comp Neurol. 2010; 518(10):1711–1723. [PubMed: 20235164]

Bruno RM, Hahn TT, Wallace DJ, de Kock CP, Sakmann B. Sensory experience alters specific branches of individual corticocortical axons during development. J Neurosci. 2009; 29(10):3172–3181. [PubMed: 19279254]

Buonomano DV, Merzenich MM. Cortical plasticity: from synapses to maps. Ann Rev Neurosci. 1998; 21:149–186. [PubMed: 9530495]

Carvell GE, Simons DJ. Abnormal tactile experience early in life disrupts active touch. J Neurosci. 1996; 16(8):2750–2757. [PubMed: 8786450]

Chen CC, Abrams S, Pinhas A, Brumberg JC. Morphological heterogeneity of layer VI neurons in mouse barrel cortex. J Comp Neurol. 2009; 512(6):726–746. [PubMed: 19065632]

Cline H, Haas K. The regulation of dendritic arbor development and plasticity by glutamatergic synaptic input: a review of the synaptotrophic hypothesis. J Physiol. 2008; 586(6):1509–1517. [PubMed: 18202093]

Crick FC, Koch C. What is the function of the claustrum? Philo Trans Roy Soc Lond Ser B: Biol Sci. 2005; 360(1458):1271–1279.

Datwani A, Iwasato T, Itohara S, Erzurumlu RS. NMDA receptor-dependent pattern transfer from afferents to postsynaptic cells and dentritic differentiation in the barrel cortex. Mol Cell Neurosci. 2002; 21(3):477–492. [PubMed: 12498788]

de Lorente Nó, R. Physiology of the nervous system. New York: Oxford University Press; 1949. Cerebral cortex: architecture, intracortical connections, motor projections; p. 288-330.

Denton DA, McKinley MJ, Farrell M, Egan GF. The role of primordial emotions in the evolutionary origin of consciousness. Conscious Cogn. 2009; 18(2):500–514. [PubMed: 18701321]

Feldman DE, Brecht M. Map plasticity in somatosensory cortex. Science. 2005; 310(5749):810–815. [PubMed: 16272113]

Fox K, Wong RO. A comparison of experience-dependent plasticity in the visual and somatosensory systems. Neuron. 2005; 48(3):465–477. [PubMed: 16269363]

Garrett JE, Wellman CL. Chronic stress effects on dendritic morphology in medial prefrontal cortex: sex differences and estrogen dependence. Neuroscience. 2009; 162(1):195–207. [PubMed: 19401219]

Hardingham N, Wright N, Dachtler J, Fox K. Sensory deprivation unmasks a PKA-dependent synaptic plasticity mechanism that operates in parallel with CaMKII. Neuron. 2008; 60(5):861–874. [PubMed: 19081380]

Harris RM, Woolsey TA. Dendritic plasticity in mouse barrel cortex following postnatal vibrissa follicle damage. J Comp Neurol. 1981; 196(3):357–376. [PubMed: 7217362]

Hickmott PW, Steen PA. Large-scale changes in dendritic structure during reorganization of adult somatosensory cortex. Nature Neurosci. 2005; 8(2):140–142. [PubMed: 15657598]

Jiao Y, Zhang C, Yanagawa Y, Sun QQ. Major effects of sensory experiences on the neocortical inhibitory circuits. J Neurosci. 2006; 26(34):8691–8701. [PubMed: 16928857]

Katz LC. Local circuitry of identified projection neurons in cat visual cortex brain slices. J Neurosci. 1987; 7(4):1223–1249. [PubMed: 3553446]

Komendantov AO, Ascoli GA. Dendritic excitability and neuronal morphology as determinants of synaptic efficacy. J Neurophysiol. 2009; 101(4):1847–1866. [PubMed: 19176614]

Kossel A, Löwel S, Bolz J. Relationships between dendritic fields and functional architecture in striate cortex of normal and visually deprived cats. J Neurosci. 1995; 15(5 Pt 2):3913–3926. [PubMed: 7538568]

Krichmar JL, Nasuto SJ, Scorcioni R, Washington SD, Ascoli GA. Effects of dendritic morphology on CA3 pyramidal cell electrophysiology: a simulation study. Brain Res. 2002; 941(1–2):11–28. [PubMed: 12031543]

Lee LJ, Chen WJ, Chuang YW, Wang YC. Neonatal whisker trimming causes long-lasting changes in structure and function of the somatosensory system. Exp Neurol. 2009; 219(2):524–532. [PubMed: 19619534]

Lee SH, Land PW, Simons DJ. Layer- and cell-type-specific effects of neonatal whisker-trimming in adult rat barrel cortex. J Neurophysiol. 2007; 97(6):4380–4385. [PubMed: 17392411]

López-Aranda MF, López-Téllez JF, Navarro-Lobato I, Masmudi-Martín M, Gutiérrez A, Khan ZU. Role of layer 6 of V2 visual cortex in object-recognition memory. Science. 2009; 325(5936):87–89. [PubMed: 19574389]

Lübke J, Albus K. The postnatal development of layer VI pyramidal neurons in the cat's striate cortex, as visualized by intracellular Lucifer yellow injections in aldehyde-fixed tissue. Brain Res: Dev Brain Res. 1989; 45(1):29–38.

Lund JS, Wu CQ. Local circuit neurons of macaque monkey striate cortex: IV. Neurons of laminae 1–3A. J Comp Neurol. 1997; 384(1):109–126. [PubMed: 9214543]

Mainen ZF, Sejnowski TJ. Influence of dendritic structure on firing pattern in model neocortical neurons. Nature. 1996; 382(6589):363–366. [PubMed: 8684467]

Maravall M, Koh IY, Lindquist WB, Svoboda K. Experience-dependent changes in basal dendritic branching of layer 2/3 pyramidal neurons during a critical period for developmental plasticity in rat barrel cortex. Cereb Cortex. 2004; 14(6):655–664. [PubMed: 15054062]

Marik SA, Yamahachi H, McManus JN, Szabo G, Gilbert CD. Axonal dynamics of excitatory and inhibitory neurons in somatosensory cortex. Plos Biology. 2010; 8(6):e1000395. [PubMed: 20563307]

McRae PA, Rocco MM, Kelly G, Brumberg JC, Matthews RT. Sensory deprivation alters aggrecan and perineuronal net expression in the mouse barrel cortex. J Neurosci. 2007; 27(20):5405–5413. [PubMed: 17507562]

Mendizabal-Zubiaga JL, Reblet C, Bueno-Lopez JL. The underside of the cerebral cortex: layer V/VI spiny inverted neurons. J Anat. 2007; 211(2):223–236. [PubMed: 17635629]

Neal JW, Winfield DA, Powell TP. The effect of visual deprivation upon the basal dendrites of Meynert cells in the striate cortex of the monkey. Philos Trans Roy Soc Lond, Ser B: Biol Sci. 1985; 225(1241):411–423.

Oray S, Majewska A, Sur M. Dendritic spine dynamics are regulated by monocular deprivation and extracellular matrix degradation. Neuron. 2004; 44(6):1021–1030. [PubMed: 15603744]

Pasternak JF, Woolsey TA. On the "selectivity" of the Golgi-Cox method. J Comp Neurol. 1975; 160(3):307–312. [PubMed: 46234]

Petersen CCH. The functional organization of the barrel cortex. Neuron. 2007; 56:339–354. [PubMed: 17964250]

Popescu MV, Ebner FF. Neonatal sensory deprivation and the development of cortical function: Unilateral and bilateral sensory deprivation result in different functional outcomes. J Neurophysiol. 2010; 104(1):98–107. [PubMed: 20427621]

Prieto JJ, Winer JA. Layer VI in cat primary auditory cortex: Golgi study and sublaminar origins of projection neurons. J Comp Neurol. 1999; 404:332–358. [PubMed: 9952352]

Rakic P. Evolution of the neocortex: a perspective from developmental biology. Nature Rev Neurosci. 2009; 10(10):724–735. [PubMed: 19763105]

Rall W, Rinzel J. Branch input resistance and steady attenuation for input to one branch of a dendritic neuron model. Biophysical J. 1973; 13(7):648–687.

Ramos RL, Tam DM, Brumberg JC. Physiology and morphology of callosal projection neurons in mouse. Neuroscience. 2008; 153(3):654–663. [PubMed: 18424008]

Rocco MM, Brumberg JC. The sensorimotor slice. J Neurosci Methods. 2007; 162(1–2):139–147. [PubMed: 17307257]

Samsonovich AV, Ascoli GA. Morphological homeostasis in cortical dendrites. PNAS. 2006; 103(5): 1569–1574. [PubMed: 16418293]

Schaefer AT, Larkum ME, Sakmann B, Roth A. Coincidence detection in pyramidal neurons is tuned by their dendritic branching pattern. J Neurophysiol. 2003; 89(6):3143–3154. [PubMed: 12612010]

Sherman SM, Guillery RW. The role of the thalamus in the flow of information to the cortex. Philos Trans Roy Soc Lond Ser B: Biol Sci. 2002; 357(1428):1695–1708. [PubMed: 12626004]

Sholl, DA. The organization of the cerebral cortex. New York: John Wiley Press; 1956.

Simons DJ, Land PW. Early experience of tactile stimulation influences organization of somatic sensory cortex. Nature. 1987; 326(6114):694–697. [PubMed: 3561512]

Sun QQ. Experience-dependent intrinsic plasticity in interneurons of barrel cortex layer IV. J Neurophysiol. 2009; 102(5):2955–2973. [PubMed: 19741102]

Sur M, Rubenstein JLR. Patterning and plasticity of the cerebral cortex. Science. 2005; 310(5749): 805–810. [PubMed: 16272112]

Tailby C, Wright LL, Metha AB, Calford MB. Activity-dependent maintenance and growth of dendrites in adult cortex. PNAS. 2005; 102(12):4631–4636. [PubMed: 15767584]

Takasaki C, Okada R, Mitani A, Fukaya M, Yamasaki M, Fujihara Y, Shirakawa T, Tanaka K, Watanabe M. Glutamate transporters regulate lesion-induced plasticity in the developing somatosensory cortex. J Neurosci. 2008; 28(19):4995–5006. [PubMed: 18463253]

Thomson AM. Neocortical layer 6, a review. Frontiers Neuroanat. 2010; 4:1–14.

Tian N, Copenhagen DR. Visual stimulation is required for refinement of ON and OFF pathways in postnatal retina. Neuron. 2003; 39(1):85–96. [PubMed: 12848934]

Trachtenberg JT, Chen BE, Knott GW, Feng G, Sanes JR, Welker E, Svoboda K. Long-term in vivo imaging of experience-dependent synaptic plasticity in adult cortex. Nature. 2002; 420(6917):788–794. [PubMed: 12490942]

Tran TS, Rubio ME, Clem RL, Johnson D, Case L, Tessier-Lavigne M, Huganir RL, Ginty DD, Kolodkin AL. Secreted semaphorins control spine distribution and morphogenesis in the postnatal CNS. Nature. 2009; 462(7276):1065–1069. [PubMed: 20010807]

Valverde, F. Golgi atlas of the postnatal mouse. Austria: Springer-Verlag; 1998.

Van der Loos H, Woolsey TA. Somatosensory cortex: structural alterations following early injury to sense organs. Science. 1973; 179(71):395–398. [PubMed: 4682966]

van Ooyen A, Duijnhouwer J, Remme MW, van Pelt J. The effect of dendritic topology on firing patterns in model neurons. Network. 2002; 13(3):311–325. [PubMed: 12222816]

White EL. Identified neurons in mouse Sml cortex which are postsynaptic to thalamocortical axon terminals: a combined Golgi-electron microscopic and degeneration study. J Comp Neurol. 1978; 181(3):627–661. [PubMed: 690279]

Woolsey TA, Dierker ML, Wann DF. Mouse SmI cortex: qualitative and quantitative classification of Golgi-impregnated barrel neurons. PNAS. 1975; 72(6):2165–2169. [PubMed: 1056021]

Zuo Y, Yang G, Kwon E, Gan WB. Long-term sensory deprivation prevents dendritic spine loss in primary somatosensory cortex. Nature. 2005; 436(7048):261–265. [PubMed: 16015331]

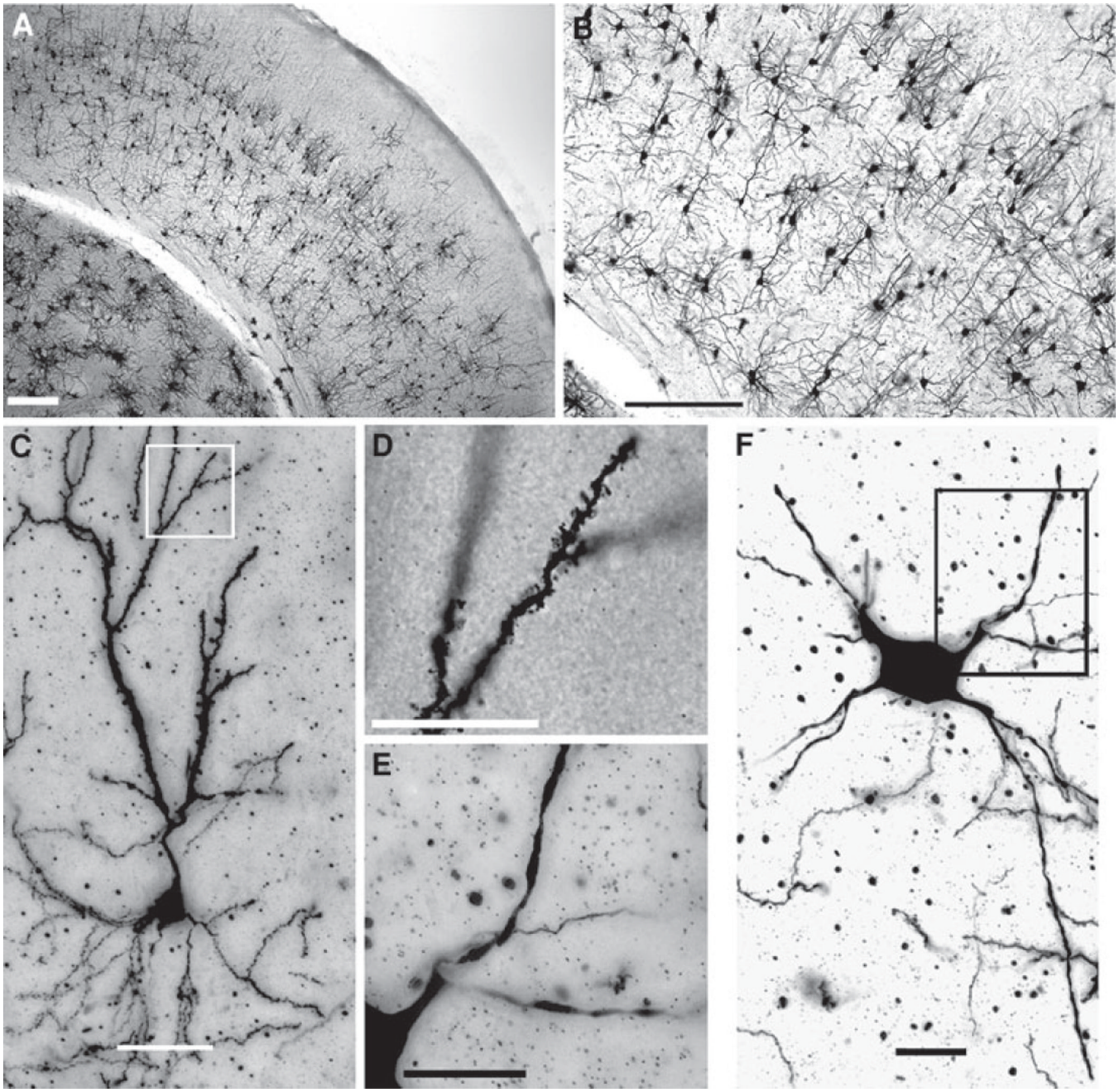

Fig. 1.

Golgi-stained section of the barrel cortex. **a** Low magnification image (×4) illustrating barrel cortex and its six distinct layers bounded by pia and the white matter. The *white box* highlights the region magnified in **b**; *Scale bar* 250 μm. **b** Higher magnification (×10) highlighting the morphologies of layer 6 (L6) neurons. *Scale bar* 250 μm. **c** Higher magnification (×20) of a single pyramidal neuron located in L6. *Scale bar* 50 μm. **d** High magnification (×100) of the region in *white* in **c**. Please note the presence of dendritic spines, demonstrating the entirety of the neuronal labeling. *Scale bar* 50 μm. **e** High magnification (×100) of the region in *black* in **f**. Please note the relative absence of dendritic

spines. *Scale bar* 25 μm. **f** ×20 magnification of a typical labeled non-pyramidal neuron located in L6. *Scale bar* 25 μm

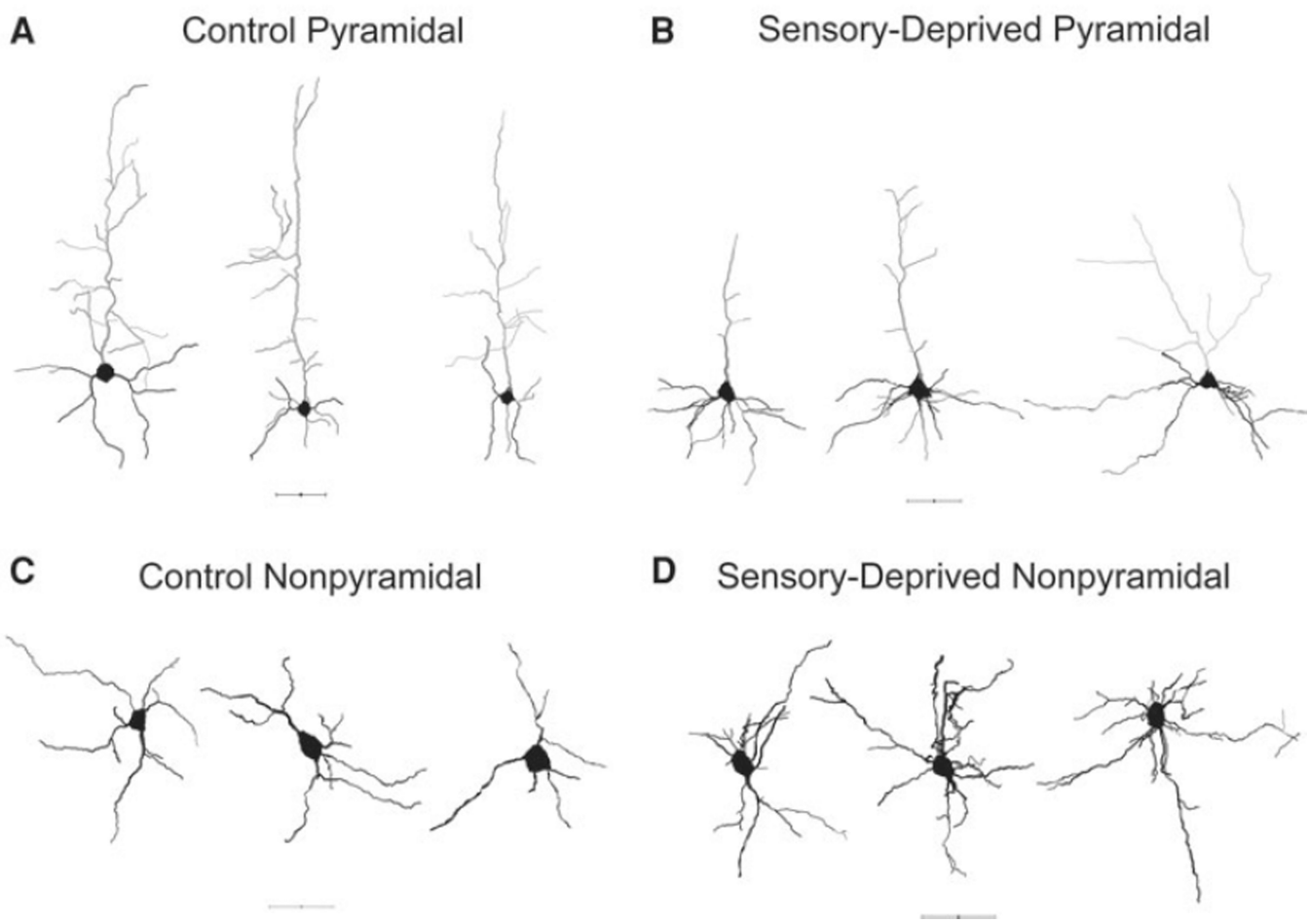

Fig. 2.

Representative reconstructed neurons. **a**, **b** Reconstructed L6 pyramidal neurons in the control P30 and sensory-deprived P30, respectively. **c**, **d** Reconstructed L6 non-pyramidal neurons in the control P30 and sensory-deprived P30, respectively. All *scale bars* 50 μm

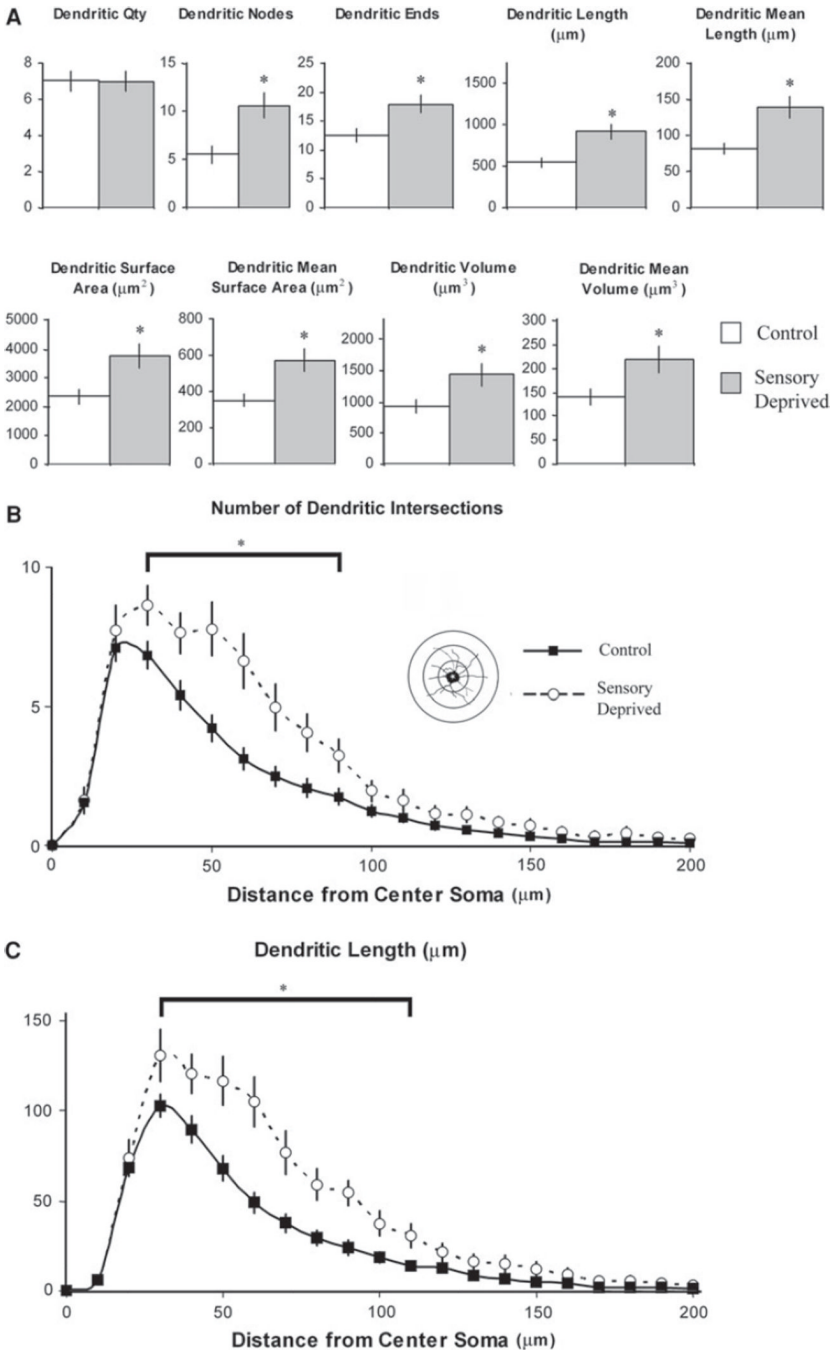

Fig. 3.

Effect of chronic sensory deprivation on dendritic parameters of L6 non-pyramidal neurons. **a** Dendritic morphometric variables in control versus sensory-deprived animals. Overall, dendritic parameters increased dramatically (with the exception of *dendritic quantity*) following chronic sensory deprivation in developing animals; means and one standard error of the mean are plotted. **b** Mean number of dendritic intersections between 10-μm concentric spheres in control versus sensory-deprived mice. Increased number of dendritic intersections in sensory-deprived relative to control mice was distributed mostly within the first 90 μm, suggesting that the effect was relatively localized. **c** Mean number of dendritic lengths

between 10-μm concentric spheres in control versus sensory-deprived mice. Similar to mean number of dendritic intersections, the increased dendritic length in sensory-deprived relative to control mice were distributed mostly within the first 110 μm of the dendrite, indicating that the effect was localized. *Error bars* indicate standard error of the mean (SEM). *Asterisks* indicates statistical significance of post hoc tests (Tukey HSD) at individual levels ($p < 0.05$)

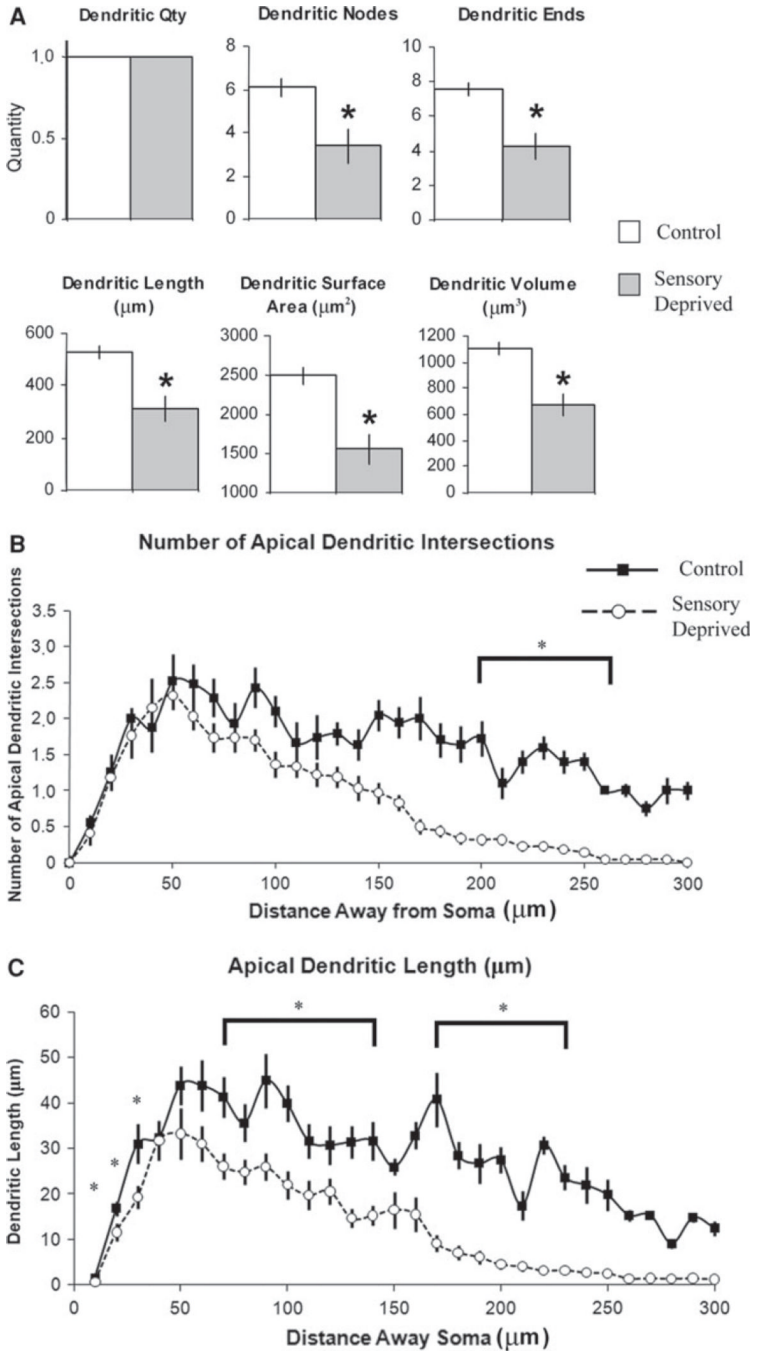

Fig. 4.

Effect of chronic sensory deprivation on apical dendritic parameters of L6 pyramidal neurons. **a** Apical dendritic morphometric variables in control versus sensory-deprived animals. Apical dendritic parameters showed significant decrease (with the exception of *dendritic quantity and number of bi/trifurcations*) following chronic sensory deprivation in developing animals; means and one standard error of the mean are plotted. **b** Mean number of apical dendritic intersections between 10-μm concentric spheres in control versus sensory-deprived mice. The decreased number of dendritic intersections in sensory-deprived relative to control mice was distributed from 120 to 180 μm from the center of the soma,

suggesting that the effect was relatively distal and might be outside of L6. **c** Mean number of apical dendritic lengths between 10-μm concentric spheres in control versus sensory-deprived mice. Similar to mean number of apical dendritic intersections, the decreased apical dendritic length in sensory-deprived relative to control mice was distributed mostly from 90 to 190 μm away from the soma. *Error bars* indicate standard error of the mean (SEM). *Asterisks* indicate statistical significance of post hoc tests (Fisher LSD) at individual levels ($p < 0.05$)

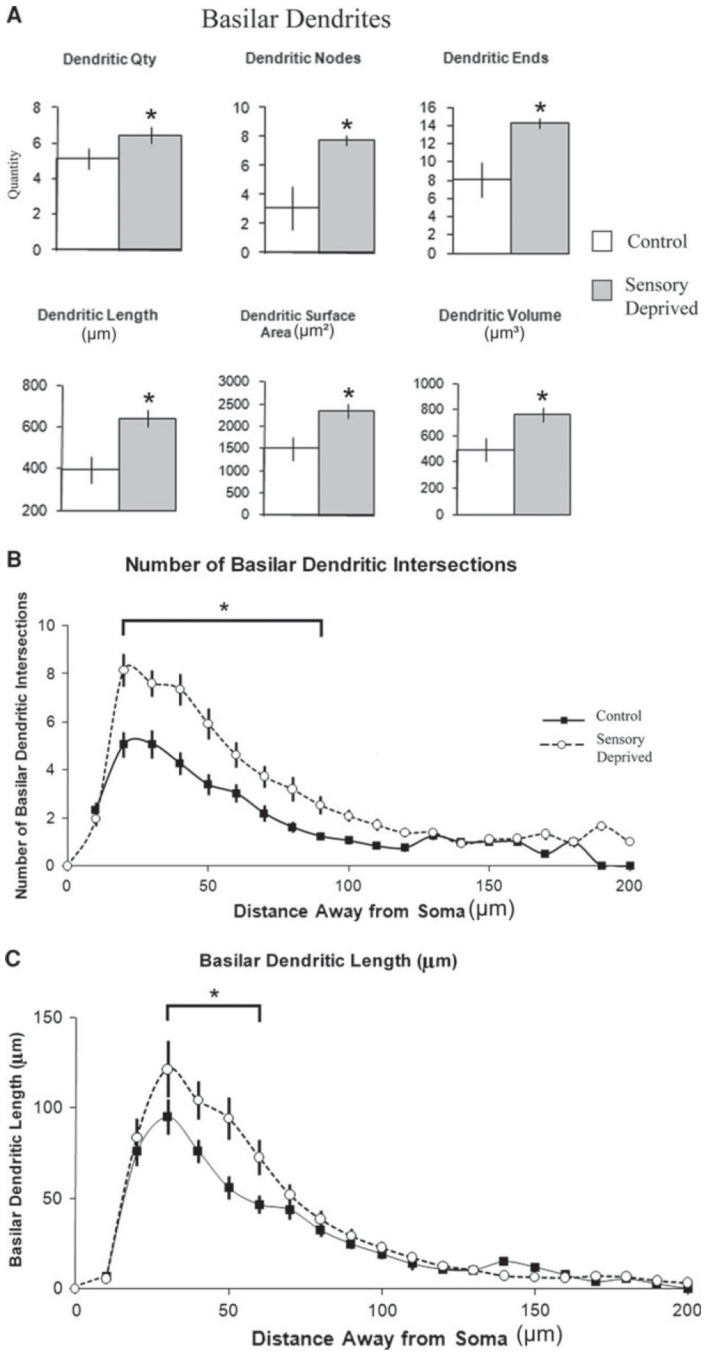

Fig. 5.

Effect of chronic sensory deprivation on basilar dendritic parameters of L6 pyramidal neurons. **a** Basilar dendritic morphometric variables in control versus sensory-deprived animals. Basilar dendritic parameters showed an overall trend to increase significantly (including *dendritic nodes, dendritic ends, and dendritic length*) following chronic sensory deprivation in developing animals; means and one standard error of the mean are plotted. **b** Mean number of basilar dendritic intersections between 10-μm concentric spheres in control versus sensory-deprived mice. The increased number of dendritic intersections in sensory-deprived relative to control mice was distributed from 20 to 50 μm away from the center of

the soma, suggesting that the effect is relatively localized. **c** Mean number of basilar dendritic lengths between 10-μm concentric spheres in control versus sensory-deprived mice. Similar to mean number of basilar dendritic intersections, the decreased basilar dendritic length in sensory-deprived relative to control animals was distributed mostly from 30 to 60 μm away from the soma, indicating the localized effect of sensory deprivation on the development of basilar dendrites. *Error bars* indicate standard error of the mean (SEM). *Asterisks* indicate statistical significance of post hoc tests (Fisher LSD) at individual levels ($p < 0.05$)

Table 1

Geometric analysis of the effect of sensory deprivation on somatic and dendritic parameters in non-pyramidal neurons

Domain	Metric	Mean sensory deprived *n* = 21	SD sensory deprived	Mean Control *n* = 35	SD control	*t* value (indep, student)	*p* value
Somatic	Perimeter (μm)	67.248	11.549	73.789	17.329	−1.56820	0.121844
Somatic	Area (μm^2)	269.869	111.833	299.603	111.547	−1.00422	0.319112
Somatic	Feret max (μm)[a]	24.614	6.008	26.609	7.102	−1.11026	0.271107
Somatic	Feret min (μm)[b]	15.076	4.059	16.150	3.092	−1.18072	0.242152
Somatic	Aspect ratio[c]	2.005	1.808	1.668	0.417	1.18366	0.240993
Somatic	Compactness[d]	0.733	0.127	0.741	0.108	−0.28795	0.774332
Somatic	Convexity[e]	0.942	0.114	0.940	0.073	0.10844	0.913995
Somatic	Form factor[f]	0.731	0.179	0.708	0.177	0.48061	0.632460
Somatic	Roundness[g]	0.552	0.160	0.561	0.158	−0.21194	0.832834
Somatic	Solidity[h]	0.950	0.026	0.923	0.085	1.43483	0.156283
Dendritic	Quantity	7.000	2.627	7.023	2.715	−0.03189	0.974664
Dendritic	Nodes *	10.619	6.144	5.523	4.577	3.74788	**0.000390**
Dendritic	Ends *	17.857	7.016	12.545	5.797	3.22497	**0.001998**
Dendritic	Length (μm) *	913.076	429.786	546.336	276.350	4.15466	**0.000100**
Dendritic	Mean length *,[i]	139.324	67.670	81.191	36.778	4.49564	**0.000030**
Dendritic	Surface area (μm^2)	3756.335	1862.085	2340.105	1188.486	3.71595	**0.000432**
Dendritic	Mean surface area *,[i]	573.962	284.364	351.255	166.751	3.97381	**0.000185**
Dendritic	Volume (μm^3) *	1433.891	864.023	926.720	555.980	2.85697	**0.005788**
Dendritic	Mean volume *,[i]	219.502	125.816	141.495	82.652	2.98811	**0.003998**

Bold indicates statistical significance at $p < 0.05$

* Statistical significance at α level preset = 0.05

[a] Feret maximum: longest diameter of the soma

[b] Feret minimum: longest diameter perpendicular to feret maximum

[c] Aspect ratio: (feret max)/(feret min); as aspect ratio approaches 1, it is indicative that the soma is closer to a symmetric shape (e.g., circle or square)

[d] Compactness: [√(4/π) × area]/(feret max); numerical values of somatic compactness closer to 1 represent a more perfect spherical soma

[e] Convexity: (convex contour)/(perimeter); this parameter is indicative of the somatic surface areal profile; higher somatic convexity yields more indentations, which translates to higher estimated surface area to cellular volume ratio

[f] Form factor: (4π × area)/(perimeter^2); this value directly reflects the complexity of somatic perimeter; a higher numerical value represents a more complex somatic perimeter

[g] Roundness: (4 × area)/(π× feret max^2), similar to compactness but is another way to differentiate objects with small compactness values for the closeness to a perfect sphere

[h] Solidity: the ratio of somata area as a whole over convex area, where values closer to 1 represent more solid (i.e., smooth, uniform) somata

[i] Dendritic mean length, mean surface area, and mean volume are all derived from total dendritic length, total surface area, and total dendritic volume divided by the number of primary dendritic trunks, respectively

Table 2

Geometric analysis of the effect of sensory deprivation on somatic, apical dendritic, and basilar dendritic parameters in pyramidal neurons

Domain	Metric	Mean sensory deprived $n = 39$	SD sensory deprived	Mean control $n = 35$	SD control	t value (indep, student)	p value
Somatic	Perimeter (μm)*	66.24	12.04	58.28	1.60	3.136	**0.001**
Somatic	Area (μm^2)*	239.88	66.16	193.90	8.39	3.351	**0.001**
Somatic	Feret max (μm)[a]	22.55	4.03	19.99	0.54	2.999	**0.002**
Somatic	Feret min (μm)[b]	16.18	3.09	14.40	0.45	2.648	**0.005**
Somatic	Aspect ratio[c]	1.4200	0.2699	1.4112	0.0383	0.151	0.440
Somatic	Compactness[d]	0.7773	0.0751	0.7904	0.0135	−0.728	0.234
Somatic	Convexity[e]	0.9379	0.0541	0.9551	0.0067	−1.554	0.062
Somatic	Form factor[f]	0.6976	0.1254	0.7286	0.0195	−1.102	0.137
Somatic	Roundness[g]	0.6098	0.1170	0.6310	0.0212	−0.753	0.227
Somatic	Solidity[h]	0.9030	0.0628	0.9191	0.0095	−1.154	0.126
Apical den.	Quantity	1	0	1	0		
Apical den.	Nodes	3.36	2.47	6.09	0.75	−3.320	**0.001**
Apical den.	Ends*	4.26	2.54	7.54	0.77	−3.902	**0.000****
Apical den.	Length (μm)*	313.97	151.02	529.87	47.66	−4.165	**0.000****
Apical den.	Surface area (μm^2)*	1553.80	713.53	2492.17	193.88	−4.272	**0.000****
Apical den.	Volume (μm^3)*	671.48	299.03	1103.80	87.67	−4.448	**0.000****
Basilar den.	Qty	6.46	3.75	5.14	0.45	1.730	**0.044**
Basilar den.	Nodes*	7.79	9.13	3.11	0.34	2.968	**0.002**
Basilar den.	Ends*	14.33	11.96	8.11	0.53	2.983	**0.002**
Basilar den.	Length (μm)*	640.78	383.28	395.06	38.00	3.314	**0.001**
Basilar den.	Mean len[i]	108.06	78.84	93.39	9.75	0.905	0.184
Basilar den.	Surface (μm^2)	2350.31	1568.56	1505.21	156.63	2.781	**0.003**
Basilar den.	Mean sur[i]	402.34	336.90	339.31	38.16	0.934	0.177
Basilar den.	Volume (μm^3)	760.09	561.90	493.98	55.60	2.449	**0.008**

Domain	Metric	Mean sensory deprived $n = 39$	SD sensory deprived	Mean control $n = 35$	SD control	t value (indep, student)	p value
Basilar den.	Mean vol[i]	131.43	120.80	110.75	13.61	0.856	0.197
Total (apical + basilar)	TD-Qty[j]	7.46	3.75	6.14	0.45	1.73	**0.044**
Total (apical + basilar)	TD-nodes[j]	11.15	10.28	9.20	0.96	0.996	0.161
Total (Apical + Basilar)	TD-ends[j]	18.59	13.05	15.66	1.09	1.203	0.117
Total (apical + basilar)	TD-length (μm)[j]	954.75	482.02	924.93	74.23	0.277	0.391
Total (apical + basilar)	TD-surface area (μm^2)[j]	3904.12	2013.13	3997.37	306.34	−0.208	0.418
Total (apical + basilar)	TD-volume[j]	1431.56	744.21	1597.78	123.80	−0.966	0.169

Bold indicates statistical significance at $p<0.05$

[*] Statistical significance at α level preset = 0.05

[**] p value less than 0.0001

[a] Feret maximum: longest diameter of the soma

[b] Feret minimum: longest diameter perpendicular to feret maximum

[c] Aspect ratio: (feret max)/(feret min); as aspect ratio approaches 1, it is indicative that the soma is closer to a symmetric shape (e.g., circle or square)

[d] Compactness: [√(4/π) × area]/(feret max); numerical values of somatic compactness closer to 1 represent a more perfect spherical soma

[e] Convexity: (convex contour)/(perimeter); this parameter is indicative of the somatic surface areal profile; higher somatic convexity yields to more indentations, which translates to higher estimated surface area to cellular volume ratio

[f] Form factor: (4π × area)/(perimeter^2); this value directly reflects the complexity of somatic perimeter; a higher numerical value represents a more complex somatic perimeter

[g] Roundness: (4 × area)/(π × feret max^2), similar to compactness but is another way to differentiate objects with small compactness values for the closeness to a perfect sphere

[h] Solidity: the ratio of somata area as a whole over convex area, where values closer to 1 represent more solid (i.e., smooth, uniform) somata

[i] Dendritic mean length, mean surface area, and mean volume: are all derived from total dendritic length, total surface area, and total dendritic volume divided by the number of primary dendritic trunks, respectively

[j] Total dendritic variables (Qty, Nodes, Ends, Length, Surface Area, Volume): These are all derived from adding apical and basilar dendritic components together, e.g., total dendritic length = apical dendritic length + basilar dendritic length